



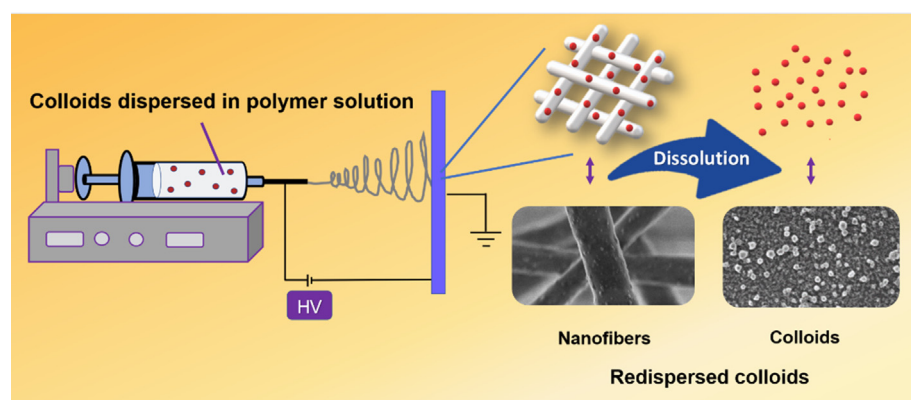
Encapsulation of emulsion droplets and nanoparticles in nanofibers as sustainable approach for their transport and storage



Chadapon Srikamut, Kusuma Thongchaivetcharat, Treethip Phakkeeree, Daniel Crespy*

Department of Materials Science and Engineering, School of Molecular Science and Engineering, Vidyasirimedhi Institute of Science and Technology (VISTEC), Rayong 21210, Thailand

GRAPHICAL ABSTRACT



ARTICLE INFO

Article history:

Received 19 March 2020
Revised 12 May 2020
Accepted 13 May 2020
Available online 22 May 2020

Keywords:

Encapsulation
Emulsion
Electrospinning
Nanofiber
Nanoparticle

ABSTRACT

Hypothesis: Emulsions are metastable and can be destabilized by coalescence and Ostwald ripening, which lead to phase separation. Immobilizing emulsion droplets in a solid material shall improve their stability during storage.

Experiments: Miniemulsions and dispersions of nanocapsules are electrospun to immobilize colloids in polymer nanofibers. The nanofibers are dissolved after various period of time to re-disperse nanodroplets and nanocapsules.

Findings: The size of nanodroplets and nanocapsules are close to the size of the original colloids before electrospinning, meaning that the emulsion droplets are efficiently stored overtime in nanofibers. Entrapping droplets in nanofibers by electrospinning allows a reduction of weight and volume of the emulsion of up to 82%. This method is therefore beneficial for improving shelf-life of emulsions, decreasing storage volume, and decreasing energy consumption for transportation of emulsions.

© 2020 Elsevier Inc. All rights reserved.

1. Introduction

Emulsions and dispersions are commonly used in cosmetics, paints, food, agriculture, and pharmaceuticals. However, storage

and transport of emulsions and dispersions are inevitably confronted with issues related to colloidal stability. For example, it is difficult for emulsions and dispersions such as beverage emulsions [1] and food colloids [2,3] to be preserved for a long period of time. Coalescence, Ostwald ripening, and flocculation are physicochemical mechanisms which impart long term stability of dispersions

* Corresponding author.

E-mail address: daniel.crespy@vistec.ac.th (D. Crespy).

[4,5]. Moreover, external factors such as vibrations during transportation of emulsions decrease their stability [6].

Pickering stabilizers have been used for improving significantly the shelf-life of emulsions [7,8]. For example, corn oil microdroplets in water were stabilized by cellulose materials and tannic acid as Pickering stabilizers [9]. After freeze-drying, the droplets could be re-dispersed in water and their sizes were similar to the droplets sizes in the original emulsion. However, this method was used for microdroplets, which are already more stable than nanodroplets. Physical methods such as spray drying [10], spray granulation [11], and freeze-drying [12] of microencapsulated liquids have been described for improving the chemical stability of emulsified liquids. However, the processes may include temperature treatments and are subjected to experimental parameters such as viscosity or droplets size and size distribution. Moreover, they can lead to coalescence of emulsion droplets and leakage of oil [13,14].

Electrospinning is a well-known technique for fabricating nanofibers. Small molecules such as drugs can be electrospun with a polymer to entrap them in nanofibrous matrix. Because of the large surface area of nanofibers, the entrapped payloads can be released very fast upon dissolution of the fibers [15–18]. Emulsion-electrospinning has been initially explored for the formation of core-sheath nanofibers because droplets can be elongated during the stretching of the electrospinning jet by the high electric field [19–24]. This feature has been used for stretching individual droplets discretely distributed in nanofibers matrix, yielding anisotropic nanoparticles after solvent evaporation [25]. Nanofibers have been used for storing droplets of hydrophobic oils [26–31] or droplets of aqueous solutions [32–36]. In the latter case, water-in-oil emulsions were electrospun in the presence of a solution of hydrophobic polymer dissolved in an organic solvent. However, water-in-oil emulsions tend to be less stable than oil-in-water emulsions and expensive block copolymers are sometimes required for their stabilization. The size of oil droplets plays a role on the morphology of fibers. Indeed, electrospinning of 6 μm -large droplets of eugenol led to a combination of core-shell and hollow fibrous structure, whereas 3 μm droplets led to the formation of core-shell structures only [36]. Coarse emulsions of toluene droplets with large size distribution were found to favor the occurrence of beads whereas emulsions with small droplet diameter (~ 200 nm) and low polydispersity could lead to the formation of homogeneous fibers [29]. Hexadecane [30], peppermint oil [31], and fish oil [26] droplets were embedded into hydrophilic polymers and the droplets could be recovered by dissolution of the fibers in water. However, the maximum loading of hexadecane, peppermint oil, and fish oil were ~ 15 wt%, 17 wt%, and 22 wt%, respectively. We demonstrate here the generality of the concept of storage and re-dispersion of emulsions by embedding emulsion droplets in various polymer nanofibers. In addition, we extended the concept to the re-dispersion of nanoparticles and nanocapsules.

2. Materials and methods

2.1. Materials

Poly(vinyl alcohol) (PVA, $M_w \sim 146,000$ – $186,000$ Da, 98.0–98.8% hydrolysis, Acros Organics), carboxymethyl cellulose, sodium salt (CMC, $M_w \sim 90,000$ Da, Acros Organics), dextran ($M_r \sim 70,000$ Da, Sigma-Aldrich), tetraethyl orthosilicate (TEOS, Acros Organics, 98%), peppermint oil (PO, Sigma-Aldrich), sodium dodecyl sulfate (SDS, 99%, Acros Organics), cetyltrimethylammonium chloride (CTMA-Cl, TCI, 95%), and *n*-hexadecane (HD, 99%, Acros Organics) were used as received. Deionized water was used throughout this work.

2.2. Preparation of the miniemulsions

Known amount of PO and 250 mg of HD were mixed and added to aqueous solutions with defined volumes and concentrations of SDS (Table S1) and stirred 1 h at 11.20 rcf. Afterwards, the emulsions were sonicated for 3 min (50% amplitude in a pulse mode with 1 s on and 1 s off) under ice-cooling.

2.3. Preparation of the dispersions

3 g of a mixture of TEOS and PO (Table S2) and 125 mg of HD were mixed with 30 g of a 0.77 wt% CTMA-Cl aqueous solution and stirred at 3.27 rcf for 10 min. The obtained emulsions were then sonicated for 3 min (50% amplitude in a pulse mode with 3 s on and 1 s off) under ice-cooling. Reactions were conducted by stirring the miniemulsions at ~ 25 °C for 20 h.

2.4. Preparation of nanofibers loaded with miniemulsion droplets

PVA solution or PVA/CMC aqueous solutions were mixed with certain amounts of PO emulsions (Table S1) to obtain dispersions with 10 wt%, 20 wt%, and 30 wt% PO containing 8 wt% PVA or 6 wt% PVA and 2 wt% CMC. Mixtures were stirred for 15 min before being transferred in 10 mL syringes with stainless steel 21G needles (0.8 mm). Nanofibers were fabricated by electrospinning at ~ 25 °C and 50–60% humidity by feeding the emulsions at a controlled flow rate of 1.5 mL/h with a syringe pump. The distance between needle and collector was 10 cm and the voltages were varied between $-10/+15$ kV, $-10/+20$ kV, $-10/+25$ kV.

2.5. Preparation of nanofibers loaded with nanoparticles (NPs) and nanocapsules (NCs)

6 g of silica nanoparticles (SiO_2NPs) or silica nanocapsules with low amount of PO ($\text{SiO}_2\text{NCs/POl}$) or silica nanocapsules with high amount of PO ($\text{SiO}_2\text{NCs/POh}$) dispersions were added to a solution 1 g dextran in 1 g water. Then, an additional 5 g of dextran was added to the dispersions and dissolved. The mixtures were transferred in 10 mL syringes with stainless steel 21G needles (0.8 mm). Nanofibers were fabricated by electrospinning at approx. 25 °C and 50–60% humidity by feeding the emulsions at a controlled flow rate of 0.3 mL/h with a syringe pump. The distance between needle and collector was 10 cm and the applied voltage was $-10/+10$ kV.

2.6. Phase separation experiments

0.8 g PVA or PVA/CMC nanofibers with embedded PO droplets were dissolved in 10 mL of a 1 mol/L AlCl_3 aqueous solution and heated at 80 °C for 15 min or at room temperature for 12 h, respectively. Consequently, nanofibers embedding PO droplets were left to settle at room temperature for 6 days.

2.7. Re-dispersion of nanodroplets, nanoparticles, and nanocapsules

10 mg of PVA or PVA/CMC nanofibers with embedded PO droplets or 10 mg dextran nanofibers with loaded SiO_2NPs or $\text{SiO}_2\text{NCs/PO}$ were dissolved in 3 g of water. PVA nanofibers with embedded PO droplets were heated at 80 °C for 5 min. PVA/CMC nanofibers with embedded PO droplets were continuously stirred at ~ 25 °C for 24 h while dextran nanofibers with loaded SiO_2NPs or $\text{SiO}_2\text{NCs/PO}$ were continuously stirred at ~ 25 °C for 2 min.

2.8. Analytical tools and instruments

Mixtures were stirred with stirring hotplates (SP88857206, Fisher Scientific) while sonication was carried out with a Branson Digital Sonifier SFX 550. Nanofibers were fabricated by electrospinning (TL-Pro-BM, Tong Li Tech) equipped with a syringe pump (TL-F6, Tong Li Tech). Hydrodynamic diameters with polydispersity index (PDI) of oil nanodroplets, silica nanoparticles, and nanocapsules were measured by dynamic light scattering (DLS, NanoPlus, Particulate systems). Weight loss in nanofibers was investigated by thermal gravimetry analysis (TGA, STA PT1600, Linseis) from 25 to 700 °C with a rate of 10 °C min⁻¹ under a nitrogen atmosphere of 100 sccm min⁻¹. Surface morphology of nanofibers, silica nanoparticles, and nanocapsules was observed with a scanning electron microscope (SEM, JSM-7610F, JEOL). The average size of nanofibers was calculated by counting 100 fibers using the ImageJ 1.52a software. X-ray diffraction (XRD) patterns of PVA fibers and PO1@PVA were investigated at 25 °C using X-ray powder diffractometer (D8 Advance, Bruker) with Cu K α radiation operated at 40 kV and 40 mA ($\lambda = 1.5406 \text{ \AA}$, data collected between 2θ of 5° to 90° with a step of 0.01°). The amount of PO nanofibers was measured by ¹H NMR spectroscopy (Bruker, 600 MHz) at 30 °C. 25 mg nanofibers were dissolved in DMSO *d*₆. To calculate the amount of PO in nanofibers, the integral of the signals between 0.66 and 0.82 ppm was selected. Because PO is a mixture of several molecules for which the signals are difficult to attribute, we constructed a calibration curve for relating the integral of the signals between 0.66 and 0.82 ppm to the concentration of PO. For this, a solution with fixed concentration of internal standard (4-hydroxybenzaldehyde, 3214 ppm) was mixed with PO at various concentrations (25000 ppm, 20143 ppm, 15000 ppm, 10000 ppm, and 5000 ppm).

3. Results and discussion

3.1. Long term stability of peppermint oil droplets

Stability of emulsions over time is a primary concern for their practical applications [1–4]. Peppermint oil (PO) was used as model oil because it is widely used in food flavors, cosmetics, and pharmaceutical products. We started hence to investigate the stability of PO droplets in water stabilized by a surfactant. PO miniemulsions were prepared with 20 wt% and 40 wt% PO and the hydrodynamic diameters of the obtained droplets were monitored with time. For miniemulsions with 20 wt% PO, the diameter increased from 175 nm (PDI = 0.145) to 388 nm (PDI = 0.157) after 45 days. During the same time, miniemulsions droplets with 40 wt% PO increased from 198 nm (PDI = 0.112) to 460 nm (PDI = 0.195) (Table 1). Emulsions were slowly destabilized due to coalescence [37] and Ostwald ripening [38]. To avoid this phenomenon, the miniemulsions were electrospun so that the droplets could be immobilized and stored in a solid matrix.

3.2. Embedding peppermint oil droplets into nanofibers

Poly(vinyl alcohol) and carboxymethyl cellulose (PVA and CMC) were selected as matrix because they are water-soluble, non-toxic,

and biocompatible [39–41]. They have been therefore electrospun and used for biomedical applications such as wound dressing [42,43], drug delivery [44–46], and tissue engineering [47]. Controlled experiments confirmed that electrospun nanofibers of pure PVA and PVA/CMC displayed a smooth surface under SEM investigation (Figs. 1a, 2a). On the contrary, the surface of PVA and PVA/CMC nanofibers electrospun under different electric fields (Table 2) and containing PO was rough, with some surface cavities (Figs. 1b–d and 2b, c). This phenomenon is typical for electrospun emulsions with discrete distribution of droplets in the nanofibers matrix [48–51].

Emulsions containing 20 wt% PO (PO1), 40 wt% PO (PO2), 60 wt% PO (PO3), and 80 wt% PO (PO4) were prepared. In the latter case, phase separation was observed immediately after emulsification by sonication so that only PO1–3 were subsequently electrospun. Hydrodynamic diameters increased from 175 to 275 nm with concentration of PO as shown in Table S1. The average diameter of the nanofibers concurrently increased from 675 ± 124 nm to 1176 ± 162 nm with amount of PO in emulsions due to larger amount of PO in fibers (Table 2). Increase of fibers diameter with increasing amount of dispersed phase was also found for PVA fibers containing fish oil [26] and retinyl palmitate [52]. We compared the XRD patterns of pure PVA fibers and PO1@PVA fibers (see Fig. S4). As expected, the strong characteristic signal of PVA was observed around $2\theta = 19.2^\circ$ [53]. The pattern for the nanofibers containing PO appears slightly broader, due to the presence of the non-crystalline PO.

For the evaluation of the stability of droplets, the fibers were dissolved in water. The hydrodynamic diameters of re-dispersed PO droplets were found to be larger, but close to the original PO droplets before electrospinning (Table 2). Indeed, at high PO loading, the average droplet diameter after re-dispersion was 279 nm (PDI = 0.148) against 275 nm (PDI = 0.207) before electrospinning. Destabilization of emulsions could be therefore prevented by their embedding in nanofibers. To understand the slight increase of PO droplets size after re-dispersion, PO1–3 emulsions were mixed with a PVA solution so that PO/PVA ratios were similar to PO/PVA ratios in the nanofibers. The diameters of PO droplets increased to 225 nm (PDI = 0.155), 263 nm (PDI = 0.135) and 348 nm (PDI = 0.139) for PO1, PO2, and PO3, respectively. Similarly, sizes of hexadecane droplets slightly increased after their re-dissolution from PVA fibers [30], indicating that PVA adsorbed on the surface of the droplets.

The PVA nanofibers were dissolved at 80 °C in water so that the dispersed phase shall not be volatile. For a more practical dissolution at lower temperatures, PVA was blended with CMC. Nanofibers with an average diameter of 365 ± 93 nm (PO1@PVA/CMC) and 918 ± 250 nm (PO2@PVA/CMC) were obtained (Table 2). Similarly to PO@PVA nanofibers, the diameters of the nanofibers increased with increasing amount of PO. PO1 and PO2 emulsions mixed with a PVA/CMC solution with the same ratio and concentration as for the electrospun dispersions displayed droplets diameters that were >100 nm larger than PO1 and PO2 droplets. The increase of diameter was larger in the presence of PVA/CMC than with PVA.

Remarkably, on the contrary to the destabilized miniemulsions monitored after 45 days, the size of the droplets stored in PVA

Table 1
Hydrodynamic diameters (D_h) of freshly prepared PO emulsion droplets in water measured by DLS and droplets after 45 days storage at 25–28 °C.

Entry	PO [wt%]	Freshly prepared PO emulsion		PO emulsion after 45 days	
		D_h [nm]	PDI	D_h [nm]	PDI
PO1	20	175	0.145	388	0.157
PO2	40	198	0.112	460	0.195

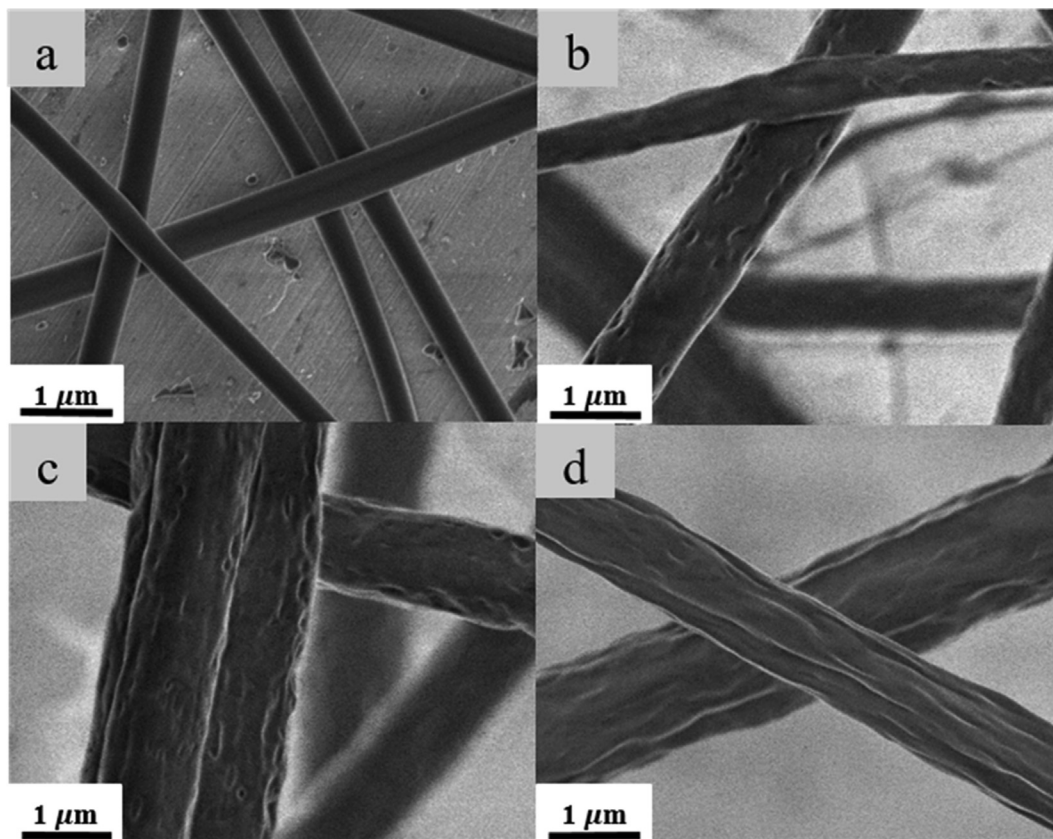


Fig. 1. SEM micrographs of a: PVA nanofibers (250 kV/m); b–d: PVA nanofibers loaded with various amounts of PO. b: PO1@PVA (56% PO, 250 kV/m); c: PO2@PVA (71% PO, 250 kV/m); d: PO3@PVA (79% PO, 300 kV/m).

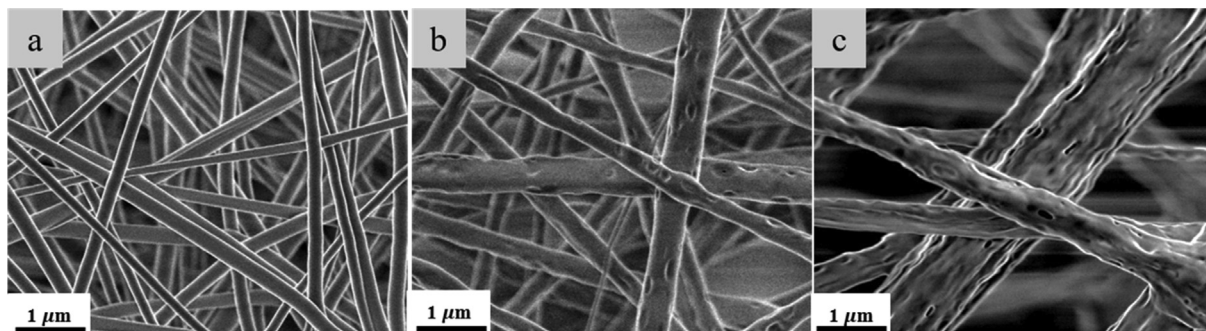


Fig. 2. SEM micrographs of a: PVA/CMC nanofibers (250 kV/m); b and c: PVA/CMC nanofibers loaded with various amounts of PO. b: PO1@PVA/CMC (56% PO, 250 kV/m); c: PO2@PVA/CMC (71% PO, 300 kV/m).

Table 2
Compositions of the fibers calculated from weighted initial amounts (PO^a) and phase separation experiments (PO^b). Diameters of the fibers measured by scanning electron microscopy (D), electrical field (nozzle-collector distance = 10 cm) (E) for producing the fibers, hydrodynamic diameters (D_h) of re-dispersed PO droplets measured by DLS.

Entry	PO^a [%]	PVA [%]	CMC [%]	E [$10^{-5}V/m$]	D [nm]	PO^b [%]	D_h	
							[nm]	PDI
PO1@PVA	55.6	44.4	0	2.5	675 ± 124	48	204	0.222
PO2@PVA	71.4	28.6	0	2.5	961 ± 163	67	266	0.130
PO3@PVA	79.0	21.0	0	3.0	1176 ± 162	71	279	0.148
PO1@PVA/CMC	55.6	33.3	11.1	2.5	365 ± 93	36	351	0.206
PO2@PVA/CMC	71.4	21.4	7.2	3.0	918 ± 250	64	325	0.228

nanofibers for 45 days was to the original size in freshly prepared emulsions. Indeed, the average diameters for 20 wt% and 40 wt% PO was measured to be 210 nm (PDI = 0.175) and 273 nm

(PDI = 0.151), respectively. Furthermore, we investigated the stability of PO1 and PO2 emulsions, and PO1@PVA and PO2@PVA nanofibers. After 7 months, phase separation in PO1 and PO2 emul-

sions were observed (see Fig. 3c). The hydrodynamic diameters of the droplets from fibers dissolved 7 months after their preparation (223 nm, PDI = 0.151; 259 nm, PDI = 0.137) were very close to the hydrodynamic diameters of droplets from fibers dissolved directly after they were prepared (204 nm, PDI = 0.222; 266 nm, PDI = 0.130).

3.3. Preservation of peppermint oil in nanofibers

To quantitatively determine the stored amount of PO, the nanofibers (PO1@PVA, PO2@PVA, PO3@PVA, PO1@PVA/CMC and PO2@PVA/CMC) were dissolved in a 1 mol/L AlCl₃ aqueous solution. AlCl₃ was chosen because the trivalent aluminum cation interacts strongly with sodium dodecyl sulfate, leading to coalescence of droplets and subsequent phase separation (Figs. 4 and 5). Weighing the upper layer yielded an almost complete recovery (85–94% recovery) of PO from PVA nanofibers (Table 2). However, visual observations indicated that the phase-separated aqueous solutions from dissolved PVA/CMC were more turbid than solutions from dissolved PVA. This induced that part of the PO was still remaining in the lower phase, hence explaining the larger discrepancies for PVA/CMC fibers between recovered PO and initial PO in the electrospinning feed.

Furthermore, we measured the quantity of PO in PVA nanofibers by ¹H NMR spectroscopy (Fig. 3a). PO1@PVA nanofibers were dissolved in DMSO-*d*₆ containing 4-hydroxybenzaldehyde as internal standard. A calibration curve (see Fig. 3b) was used for calculating the amount of PO, which was 89% of the initial amount of PO in the electrospinning feed. This means that most of PO remain in the nanofibers.

Because most of the oil is preserved in the nanofibers, electrospinning of emulsion can be considered as a method for storing emulsion nanodroplets for long periods of time. This type of storage is beneficial for reducing energy of transportation of emulsions because the weight of the nanofibers is lower than the weight of the emulsions. The reduction in weight can be calculated by $\Delta m = (m_{\text{initial}} - m_{\text{final}})/m_{\text{initial}}$. m_{initial} is the weight of the electrospinning dispersion containing PVA, water, and PO. m_{final} is the weight of PO and PVA because water evaporated. For PO1@PVA nanofibers, the amount of water is 82 wt% and therefore the reduction in weight is also 82 wt%.

3.4. Thermal stability of nanofibers

Thermal gravimetric analysis (TGA) of the nanofibers was performed to investigate the thermal stability of the nanofibers (Fig. S1–S2). TGA thermogram of pure PVA nanofibers (NFP) displayed three weight loss stages that could be identified to residual moisture (40–100 °C), degradation of PVA side chains (200–350 °C), and degradation of PVA main chain (380–530 °C) (Fig. S1) [54]. Weight loss for PVA and PVA/CMC nanofibers containing PO also occurred in 3 stages (Fig. S1–S2). However, the first stage was extended to higher temperatures (till 230 °C) and also included evaporation of PO.

3.5. Embedding and releasing nanoparticles and nanocapsules in nanofibers

To generalize the concept of storage of emulsions to other types of dispersion, we electrospun SiO₂NPs and SiO₂NCs/PO embedded in fibers. Dextran was selected as nanofibers matrix due to its high

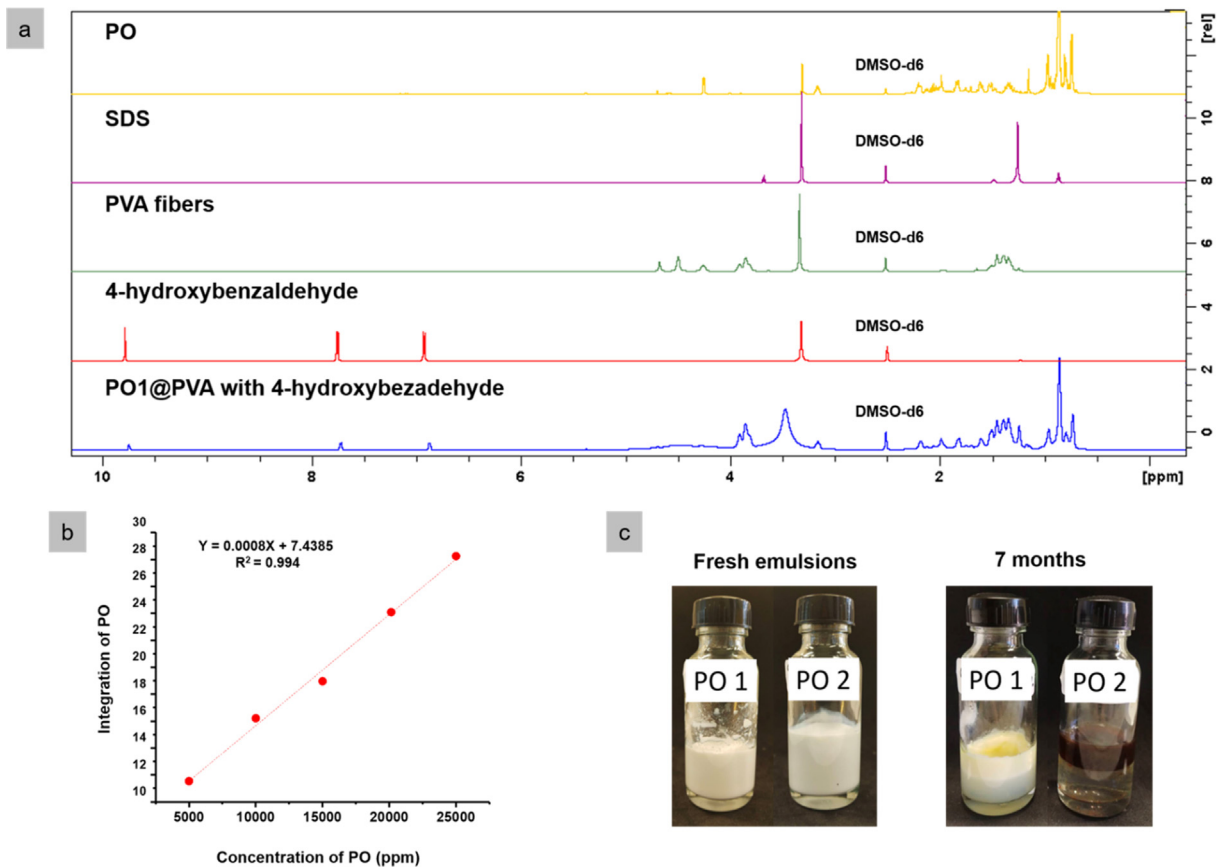


Fig. 3. a: ¹H NMR spectra of a: PO, SDS, PVA fibers, 4-hydroxybenzaldehyde, and PO1@PVA with 4-hydroxybenzaldehyde in DMSO-*d*₆. b: calibration curve for determining PO concentration calculated from integration of ¹H NMR signals for PO (0.66–0.82 ppm) and the internal standard signal 4-hydroxybenzaldehyde (9.77 ppm). c: photographs of freshly prepared PO1 and PO2 emulsions and the same emulsions after 7 months of storage at 25–28 °C.

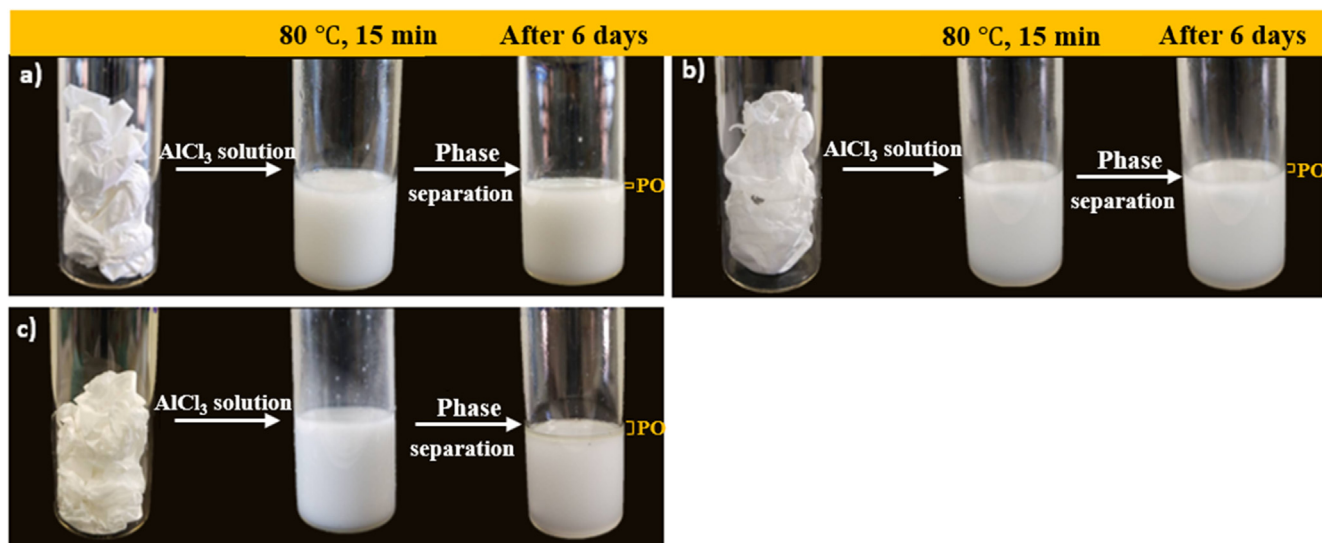


Fig. 4. Photographs of non-woven fibers of a–d: PVA nanofibers loaded with various amounts of PO. a: PO1@PVA (56% PO, 250 kV/m); b: PO2@PVA (71% PO, 250 kV/m); c: PO3@PVA (79% PO, 300 kV/m), their dissolution in AlCl_3 aqueous solutions, followed by phase separation after 6 days.

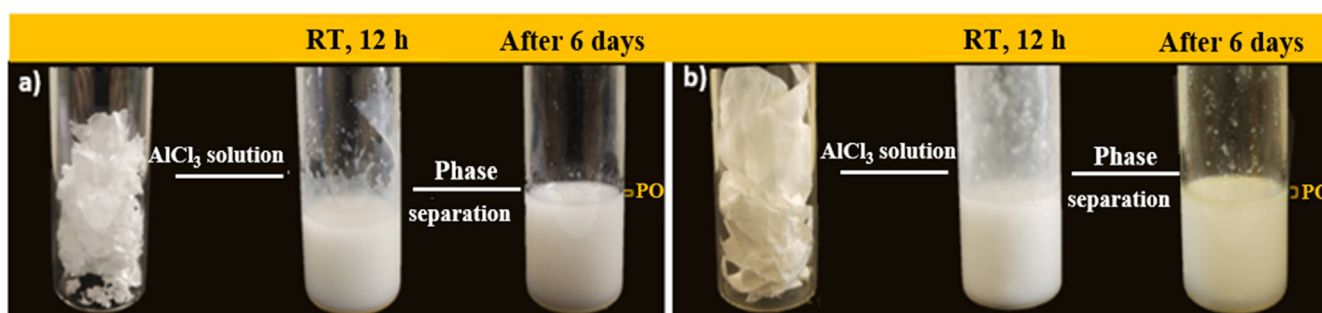


Fig. 5. Photographs of non-woven fibers of a–c: PVA mixed CMC nanofibers loaded with various amounts of PO. a: PO1@PVA/CMC (56% PO, 250 kV/m); b: PO2@PVA/CMC (71% PO, 300 kV/m), their dissolution in AlCl_3 aqueous solution, followed by phase separation after 6 days.

solubility in water and biocompatibility. Moreover, it no needs to use high temperature and long period of time for dissolving the nanofibers. Nanocapsules were formed by a sol–gel process confined at the interface of miniemulsion droplets so that PO could be encapsulated by a thin silica shell [55]. The presence of the colloids could be observed on the rough surface of nanofibers by SEM (Fig. 6b, e, h). Interestingly, the morphology of SiO_2 NPs and SiO_2 -NCs/PO after dissolving the fibers (Fig. 6c, f, i) was similar with their morphology before electrospinning (Fig. 6a, d, g). Furthermore, the hydrodynamic diameter of SiO_2 NPs and SiO_2 NCs/PO before electrospinning and after dissolution of the fibers were found to be very close (Table S2).

4. Conclusions

Nanofibers containing various amounts of immobilized droplets in a polymer matrix could be prepared by electrospinning oil-in-water emulsions. Our hypothesis was that high amount of emulsion droplets could be stored in fibers by electrospinning because the continuous phase is evaporated during the process. Emulsion droplets could be recovered by dissolving the nanofibers, even after long time. The droplets sizes were close to the original ones before electrospinning. Furthermore, SiO_2 NPs and SiO_2 NCs/PO could be re-dispersed after being embedded in nanofibers. Entrapment of emulsion droplets in nanofibers could be used as storage method for saving space during storage and transportation. Reduc-

tion in weight to up to 82% of the original emulsion could be achieved in the PO1@PVA nanofibers. Furthermore, spinning emulsions can save energy because they require less energy to be transported. Typical energy required for the transportation of food by trucks in the USA is estimated to be $2.7 \text{ MJ} \cdot \text{t}^{-1} \cdot \text{km}^{-1}$ [56]. Pickering stabilizers have been used for improving the shelf life of emulsions. For example, corn oil microdroplets ($\sim 3\text{--}4 \mu\text{m}$) stabilized by cellulose nanocrystals and tannic acid could be re-dispersed in water after freeze-drying [9]. Physical methods such as spray drying, spray granulation, and freeze-drying were also studied for prolongating the stability of emulsions. These methods were compared for the storage of fish oil [11]. The encapsulation efficiency of fish oil was around 96% for spray granulation, 84% for spray drying, and less than 50% for the freeze-drying process. Although longer residence time was needed for spray granulation, materials prepared by this method offered also the highest resistance against oxidation of fish oil. Indeed, spray drying occurred at $80\text{--}180 \text{ }^\circ\text{C}$ and the powder obtained by freeze-drying was porous, leading to a faster oxidation of the oil. Moreover, it is known that freeze-drying of core-shell particles can lead to leakage of oil because of possible breakage of the polymer shell during the freezing step [57].

To overcome the drawbacks of conventional methods such as long residence time, leakage, or the use of temperature and pressure, nanofibers containing various amounts of immobilized droplets in a polymer matrix were prepared by electrospinning oil-in-water emulsions. Hexadecane and fish oil nanodroplets were already embedded into PVA nanofibers, but with a maximum con-

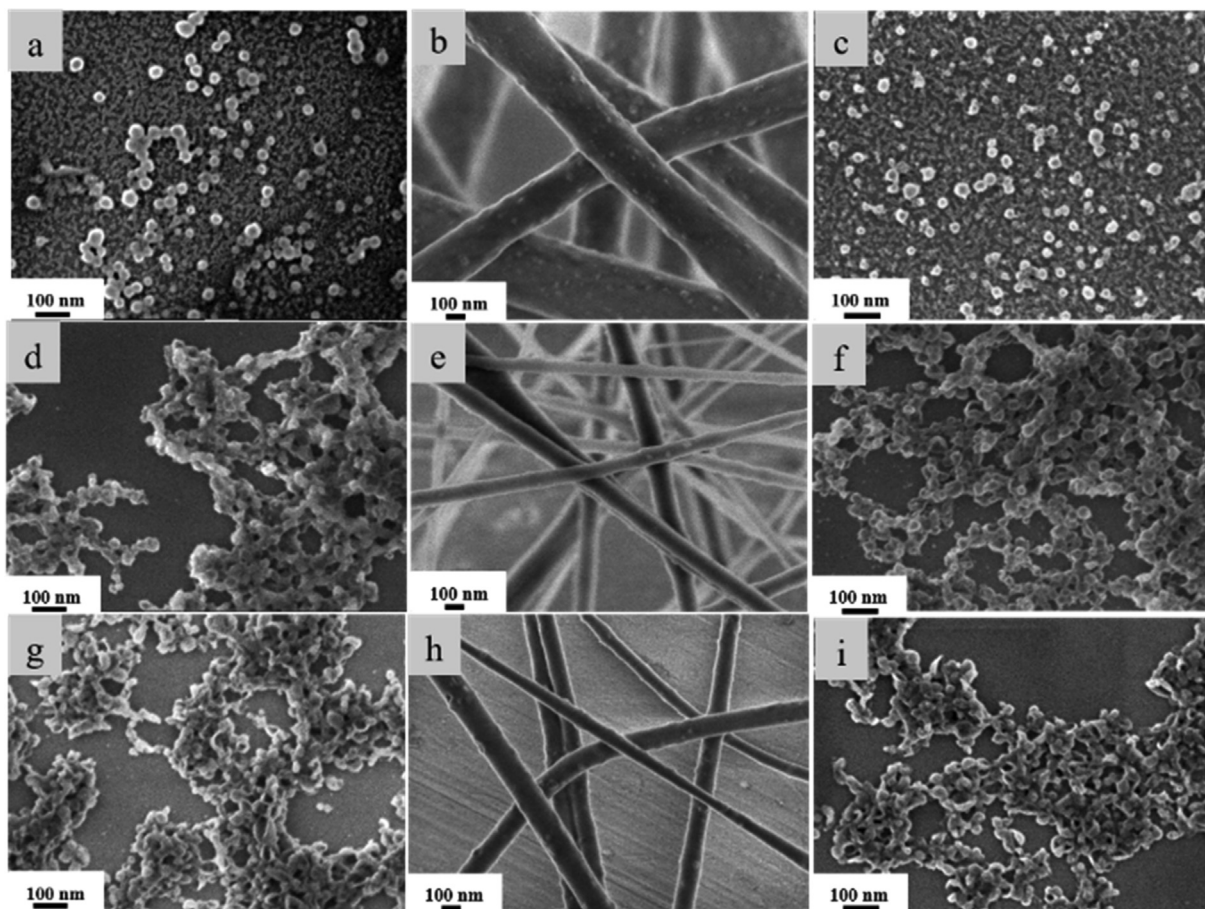


Fig. 6. SEM micrographs of a–c: SiO₂NPs (w:w TEOS:PO = 100:0); d–f: SiO₂ NCs/POI (TEOS:PO = 83:17); g–i: SiO₂ NCs/POh (TEOS:PO = 67:33) – a, d, g: before electrospinning in dextran fibers; b, e, h: embedded in dextran fibers; c, f, i: after dissolving the loaded dextran fibers in water.

tent ~15 wt% [26] and 22 wt% [30], respectively. Similarly, a maximum of 17 wt% PO nanodroplets were embedded into dextran nanofibers [31]. Herein, up to 70 wt% liquid droplets of essential oil could be stored in PVA or blends of PVA and CMC and then re-dispersed. It is of interest for future work to develop this method further for storing aqueous droplets of water-in-oil emulsions.

CRediT authorship contribution statement

Chadapon Srikamut: Methodology, Conceptualization, Formal analysis, Visualization, Investigation, Writing - original draft.
Kusuma Thongchaivetcharat: Formal analysis, Investigation.
Treethip Phakkeeree: Formal analysis, Investigation, Supervision.
Daniel Crespy: Conceptualization, Writing - review & editing, Supervision.

Declaration of Competing Interest

The authors declare that they have no known competing financial interests or personal relationships that could have appeared to influence the work reported in this paper.

Acknowledgements

This work was supported by the Vidyasirimedhi Institute of Science and Technology (VISTEC) and the Office of the Higher Education Commission of Thailand (OHEC). T.P. appreciates the Post-

doctoral Fellowship of the Vidyasirimedhi Institute of Science and Technology. Instrumental support from the Frontier Research Center (FRC) at VISTEC is also acknowledged.

Appendix A. Supplementary data

Supplementary data to this article can be found online at <https://doi.org/10.1016/j.jcis.2020.05.056>.

References

- [1] R.A. Buffo, G.A. Reineccius, Shelf-life and mechanisms of destabilization in dilute beverage emulsions, *Flavour Fragr. J.* 16 (2001) 7–12.
- [2] E. Dickinson, V.B. Galazka, Emulsion stabilization by ionic and covalent complexes of β -lactoglobulin with polysaccharides, *Food Hydrocoll.* 5 (1991) 281–296.
- [3] S. Tcholakova, N.D. Denkov, I.B. Ivanov, B. Campbell, Coalescence stability of emulsions containing globular milk proteins, *Adv. Colloid Interface Sci.* 123–126 (2006) 259–293.
- [4] E. Fredrick, P. Walstra, K. Dewettinck, Factors governing partial coalescence in oil-in-water emulsions, *Adv. Colloid Interface Sci.* 153 (2010) 30–42.
- [5] D.E. Tambe, M.M. Sharma, Factors controlling the stability of colloid-stabilized emulsions: I. An experimental investigation, *J. Colloid Interface Sci.* 157 (1993) 244–253.
- [6] B. Liu, W. Hou, Influence of storage conditions on the stability of asphalt emulsion, *Pet. Sci. Technol.* 35 (2017) 1217–1223.
- [7] R. Aveyard, B. Binks, J. Clint, Emulsions stabilised solely by colloidal particles, *Adv. Colloid Interface Sci.* 100 (2003) 503–546.
- [8] T. Chen, P.J. Colver, S.A.F. Bon, Organic-inorganic hybrid hollow spheres prepared from TiO₂-stabilized Pickering emulsion polymerization, *Adv. Mater.* 19 (2007) 2286–2289.
- [9] Z. Hu, H.S. Marway, H. Kasem, R. Pelton, E.D. Cranston, Dried and redispersible cellulose nanocrystal pickering emulsions, *ACS Macro Lett.* 5 (2016) 185–189.

- [10] A. Gharsallaoui, G. Roudaut, O. Chambin, A. Voilley, R. Saurel, Applications of spray-drying in microencapsulation of food ingredients: an overview, *Food Res. Int.* 40 (2007) 1107–1121.
- [11] S.H. Anwar, B. Kunz, The influence of drying methods on the stabilization of fish oil microcapsules: comparison of spray granulation, spray drying, and freeze drying, *J. Food Eng.* 105 (2011) 367–378.
- [12] K. Heinzelmann, K. Franke, Using freezing and drying techniques of emulsions for the microencapsulation of fish oil to improve oxidation stability, *Colloids Surf. B* 12 (1999) 223–229.
- [13] P. Fäldt, B. Bergenstahl, Fat encapsulation in spray-dried food powders, *J. Am. Oil Chem. Soc.* 72 (1995) 171–176.
- [14] M. Cerdeira, S. Martini, M. Herrera, Microencapsulating properties of trehalose and of its blends with sucrose and lactose, *J. Food Sci.* 70 (2006) e401–e408.
- [15] D.-G. Yu, X.-X. Shen, C. Branford-White, K. White, L.-M. Zhu, S.W. Annie Bligh, Oral fast-dissolving drug delivery membranes prepared from electrospun polyvinylpyrrolidone ultrafine fibers, *Nanotechnology* 20 (2009) 055104.
- [16] X. Li, M.A. Kanjwal, L. Lin, I.S. Chronakis, Electrospun polyvinyl-alcohol nanofibers as oral fast-dissolving delivery system of caffeine and riboflavin, *Colloids Surf. B* 103 (2013) 182–188.
- [17] Z.K. Nagy, K. Nyul, I. Wagner, K. Molnar, G. Marosi, Electrospun water soluble polymer mat for ultrafast release of Donepezil HCl, *Express Polym. Lett.* 4 (2010) 763–772.
- [18] Q. Wang, D.-G. Yu, L.-L. Zhang, X.-K. Liu, Y.-C. Deng, M. Zhao, Electrospun hypromellose-based hydrophilic composites for rapid dissolution of poorly water-soluble drug, *Carbohydr. Polym.* 174 (2017) 617–625.
- [19] X. Xu, L. Yang, X. Xu, X. Wang, X. Chen, Q. Liang, J. Zeng, X. Jing, Ultrafine medicated fibers electrospun from w/o emulsions, *J. Control. Release* 108 (2005) 33–42.
- [20] H. Qi, P. Hu, J. Xu, A. Wang, Encapsulation of drug reservoirs in fibers by emulsion electrospinning: morphology characterization and preliminary release assessment, *Biomacromolecules* 7 (2006) 2327–2330.
- [21] A.L. Yarin, Coaxial electrospinning and emulsion electrospinning of core-shell fibers, *Polym. Adv. Technol.* 22 (2011) 310–317.
- [22] N. Nikmaram, S. Roohinejad, S. Hashemi, M. Koubaa, F.J. Barba, A. Abbaspourrad, R. Greiner, Emulsion-based systems for fabrication of electrospun nanofibers: food, pharmaceutical and biomedical applications, *RSC Adv.* 7 (2017) 28951–28964.
- [23] C. Wang, L. Wang, M. Wang, Evolution of core-shell structure: From emulsions to ultrafine emulsion electrospun fibers, *Mater. Lett.* 124 (2014) 192–196.
- [24] S. Jiang, L.-P. Lv, K. Landfester, D. Crespy, Nanocontainers in and onto nanofibers, *Acc. Chem. Res.* 49 (2016) 816–823.
- [25] C. Herrmann, A. Turshatov, D. Crespy, Fabrication of polymer ellipsoids by the electrospinning of swollen nanoparticles, *ACS Macro Lett.* 1 (2012) 907–909.
- [26] P.J. García-Moreno, K. Stephansen, J. van der Kruijs, A. Guadix, E.M. Guadix, I.S. Chronakis, C. Jacobsen, Encapsulation of fish oil in nanofibers by emulsion electrospinning: physical characterization and oxidative stability, *J. Food Eng.* 183 (2016) 39–49.
- [27] C. Krieger, K.M. Kit, D.J. McClements, J. Weiss, Nanofibers as carrier systems for antimicrobial microemulsions Part I: fabrication and characterization, *Langmuir* 25 (2009) 1154–1161.
- [28] M.W. Lee, S. An, C. Lee, M. Liou, A.L. Yarin, S.S. Yoon, Hybrid self-healing matrix using core-shell nanofibers and capsuleless microdroplets, *ACS Appl. Mater. Interfaces* 6 (2014) 10461–10468.
- [29] A. Kaltbeitzel, K. Friedemann, A. Turshatov, C. Schönecker, I. Lieberwirth, K. Landfester, D. Crespy, STED analysis of droplet deformation during emulsion electrospinning, *Macromol. Chem. Phys.* 218 (2017) 1600547.
- [30] A. Arecchi, S. Mannino, J. Weiss, Electrospinning of poly(vinyl alcohol) nanofibers loaded with hexadecane nanodroplets, *J. Food Sci.* 75 (2010) N80–N88.
- [31] K. Thongchaivetcharat, R. Jenjob, D. Crespy, Encapsulation and release of functional nanodroplets entrapped in nanofibers, *Small* 14 (2018) 1704527.
- [32] M. Buzgo, E. Filova, A.M. Staffa, M. Rampichova, M. Doupnik, K. Vocetkova, V. Lukasova, R. Kolcun, D. Lukas, A. Necas, E. Amler, Needleless emulsion electrospinning for the regulated delivery of susceptible proteins, *J. Tissue Eng. Regen. Med.* 12 (2018) 583–597.
- [33] E.H. Sanders, R. Kloefkorn, G.L. Bowlin, D.G. Simpson, G.E. Wnek, Two-phase electrospinning from a single electrified jet: Microencapsulation of aqueous reservoirs in poly(ethylene-co-vinyl acetate) fibers, *Macromolecules* 36 (2003) 3803–3805.
- [34] D. Yang, Y. Li, J. Nie, Preparation of gelatin/PVA nanofibers and their potential application in controlled release of drugs, *Carbohydr. Polym.* 69 (2007) 538–543.
- [35] J. Pal, D. Wu, M. Hakkarainen, R.K. Srivastava, The viscoelastic interaction between dispersed and continuous phase of PCL/HA-PVA oil-in-water emulsion uncovers the theoretical and experimental basis for fiber formation during emulsion electrospinning, *Eur. Polym. J.* 96 (2017) 44–54.
- [36] Y. Li, F.K. Ko, W.Y. Hamad, Effects of emulsion droplet size on the structure of electrospun ultrafine biocomposite fibers with cellulose nanocrystals, *Biomacromolecules* 14 (2013) 3801–3807.
- [37] K. Boode, P. Walstra, Partial coalescence in oil-in-water emulsions 1. Nature of the aggregation, *Colloids Surf. A Physicochem. Eng. Asp.* 81 (1993) 121–137.
- [38] P. Taylor, Ostwald ripening in emulsions, *Adv. Colloid Interface Sci.* 75 (1998) 107–163.
- [39] G. Paradossi, F. Cavalieri, E. Chiessi, C. Spagnoli, M.K. Cowman, Poly(vinyl alcohol) as versatile biomaterial for potential biomedical applications, *J. Mater. Sci. Mater. Med.* 14 (2003) 687–691.
- [40] B. Ding, H.-Y. Kim, S.-C. Lee, D.-R. Lee, K.-J. Choi, Preparation and characterization of nanoscaled poly(vinyl alcohol) fibers via electrospinning, *Fibers Polym.* 3 (2002) 73–79.
- [41] T. Miyamoto, S.-I. Takahashi, H. Ito, H. Inagaki, Y. Noishiki, Tissue biocompatibility of cellulose and its derivatives, *J. Biomed. Mater. Res.* 23 (1989) 125–133.
- [42] Y. Zhou, D. Yang, X. Chen, Q. Xu, F. Lu, J. Nie, Electrospun water-soluble carboxyethyl chitosan/poly(vinyl alcohol) nanofibrous membrane as potential wound dressing for skin regeneration, *Biomacromolecules* 9 (2008) 349–354.
- [43] S. Kim, S.-G. Park, S.-W. Kang, K.J. Lee, Nanofiber-based hydrocolloid from colloid electrospinning toward next generation wound dressing, *Macromol. Mater. Eng.* 301 (2016) 818–826.
- [44] M.H. El-Newehy, M.E. El-Naggar, S. Alotaiby, H. El-Hamshary, M. Moydeen, S. Al-Deyab, Preparation of biocompatible system based on electrospun CMC/PVA nanofibers as controlled release carrier of diclofenac sodium, *J. Macromol. Sci. A* 53 (2016) 566–573.
- [45] E.A. Krogstad, K.A. Woodrow, Manufacturing scale-up of electrospun poly(vinyl alcohol) fibers containing tenofovir for vaginal drug delivery, *Int. J. Pharm.* 475 (2014) 282–291.
- [46] A. Esmaili, M. Haseli, Optimization, synthesis, and characterization of coaxial electrospun sodium carboxymethyl cellulose-graft-methyl acrylate/poly(ethylene oxide) nanofibers for potential drug-delivery applications, *Carbohydr. Polym.* 173 (2017) 645–653.
- [47] H. Ghasemi Hamidabadi, Z. Rezvani, M. Nazm Bojnordi, H. Shirinzadeh, A.M. Seifalian, M.T. Joghataei, M. Razaghpour, A. Alibakhshi, A. Yazdanpanah, M. Salimi, M. Mozafari, A.M. Urbanska, R.L. Reis, S.C. Kundu, M. Gholipourmalekabadi, Chitosan-intercalated montmorillonite/poly(vinyl alcohol) nanofibers as a platform to guide neuronlike differentiation of human dental pulp stem cells, *ACS Appl. Mater. Interfaces* 9 (2017) 11392–11404.
- [48] S. Yan, L. Xiaoqiang, L. Shuiping, M. Xiumei, S. Ramakrishna, Controlled release of dual drugs from emulsion electrospun nanofibrous mats, *Colloids Surf. B* 73 (2009) 376–381.
- [49] C.A. Carrillo, T. Nypelö, O.J. Rojas, Double emulsions for the compatibilization of hydrophilic nanocellulose with non-polar polymers and validation in the synthesis of composite fibers, *Soft Matter* 12 (2016) 2721–2728.
- [50] L. Zhao, J. Luo, Y. Li, H. Wang, G. Song, G. Tang, Emulsion-electrospinning *n*-octadecane/silk composite fiber as environmental-friendly form-stable phase change materials, *J. Appl. Polym. Sci.* 134 (2017) 45538.
- [51] G. Yazgan, A.M. Popa, R.M. Rossi, K. Maniura-Weber, J. Puigmartí-Luis, D. Crespy, G. Fortunato, Tunable release of hydrophilic compounds from hydrophobic nanostructured fibers prepared by emulsion electrospinning, *Polymer* 66 (2015) 268–276.
- [52] V. Gordon, G. Marom, S. Magdassi, Formation of hydrophilic nanofibers from nanoemulsions through electrospinning, *Int. J. Pharm.* 478 (2015) 172–179.
- [53] R. Ricciardi, F. Auriemma, C. De Rosa, F. Lauprêtre, X-ray diffraction analysis of poly(vinyl alcohol) hydrogels, obtained by freezing and thawing techniques, *Macromolecules* 37 (2004) 1921–1927.
- [54] Z. Peng, L.X. Kong, A thermal degradation mechanism of polyvinyl alcohol/silica nanocomposites, *Polym. Degrad. Stab.* 92 (2007) 1061–1071.
- [55] A. Jobdeedamrong, R. Jenjob, D. Crespy, Encapsulation and release of essential oils in functional silica nanocontainers, *Langmuir* 34 (2018) 13235–13243.
- [56] C.L. Weber, H.S. Matthews, Food-miles and the relative climate impacts of food choices in the united states, *Environ. Sci. Technol.* 42 (2008) 3508–3513.
- [57] M.J. Choi, S. Briançon, J. Andrieu, S.G. Min, H. Fessi, Effect of freeze-drying process conditions on the stability of nanoparticles, *Dry. Technol.* 22 (2004) 335–346.